Journal of Electronic Materials (2022) 51:684–691
https://doi.org/10.1007/s11664-021-09323-7

ORIGINAL RESEARCH ARTICLE

Properties of Multiwalled Carbon Nanotube-Reinforced Alumina Composites Produced Following the Sol-Spray Technique

Songlin Tan[1] · Rui Bao[1] · Yongqi Zhuang[1] · Jianhong Yi[1]

Received: 1 September 2021 / Accepted: 27 October 2021 / Published online: 29 November 2021

Abstract

Multi-wall carbon nanotube (MWNT)-reinforced alumina composites were prepared by a sol-spray process combined with a vacuum hot press process. The relative densities of all the samples were higher than 97%. Scanning electron microscopy (SEM) results showed that the MWNTs were well-dispersed in the alumina matrix; specifically, most of them were distributed along the grain boundaries in the form of networks, whereas the others were located in the grains. For 0.5 wt.% MWNTs, the Vicker hardness and fracture toughness were 32.1% and 75.6% higher than those of pure alumina, and the average increment of the thermal diffusivity under different test temperatures is ~ 26.2%. When the content of MWNTs is higher than 0.5 wt.%, the composites showed conductor properties. Moreover, the percolation threshold of the prepared composites was 0.37 wt.% with the nonlinear fitting of conductivity data, which indicates that the MWNTs were well dispersed in the alumina matrix.

Graphical Abstract

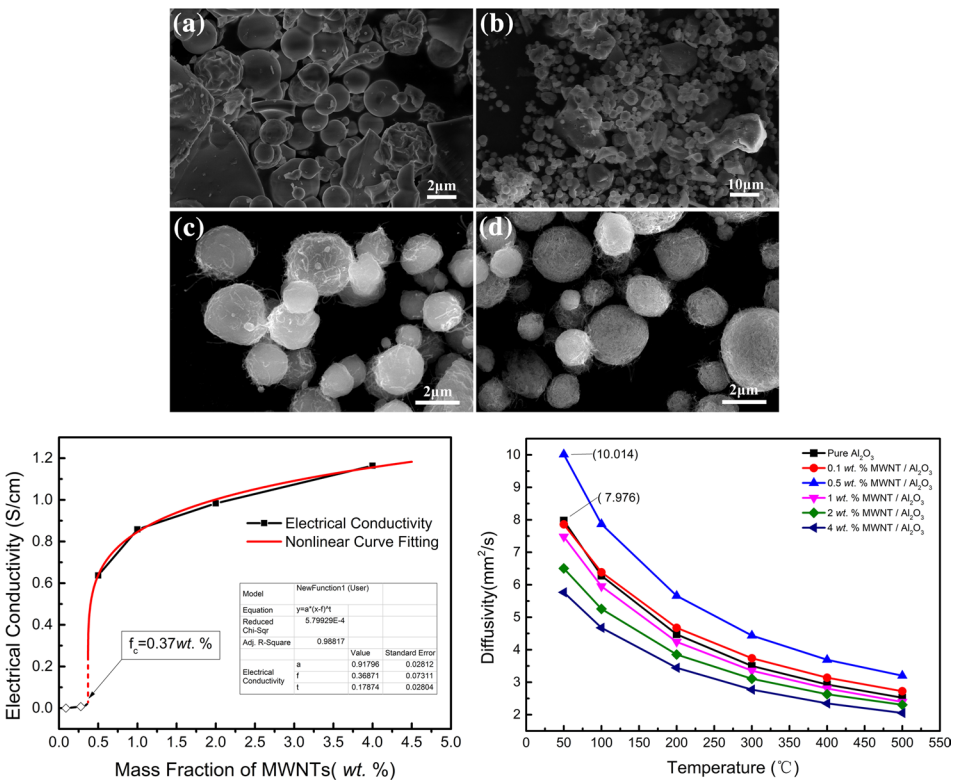

Keywords Carbon nanotubes · alumina · sol-spray · composites · well dispersion

Extended author information available on the last page of the article

Introduction

Carbon nanotubes (CNTs), also known as buckytubes, were found experimentally by the Japanese scientist Iijima in 1991. CNTs are ideal engineering materials that can be used for the fabrication of nanoelectronics, sensors, etc., due to their excellent mechanical, electrical, and thermal properties.[1,2] Introducing them to polymer, metal, and ceramic matrices enhances the mechanical, electrical, thermal, and photocatalytic properties. They have become an important topic of research in functional composite materials.[3,4] It is well known that alumina is widely used as an engineering structural material in various high-temperature and high-pressure application environments due to its excellent mechanical properties and thermal and chemical stability. It can also be used under acidic or alkaline conditions to develop ceramic bearings, electronic substrates, spark plugs, insulation materials, and magnetohydrodynamic generators.[5] However, when it comes to the functional material in heating elements, electronic igniters, electromagnetic and anti-static shielding of electronic elements, fuel cell electrodes, crucibles, electrical penetration assemblies of vacuum induction furnaces, etc., higher electrical and thermal conductivities of the alumina matrix are required.[6–8] Generally, metal particles are always employed to improve the insulating ceramic material's electrical and thermal properties. Just like metal additives, CNTs with excellent mechanical, electrical, and thermal properties can also enhance the properties of ceramic materials.[9–11] In addition, it has been reported that multi-wall carbon nanotubes (MWNTs) can conduct electricity even at low temperatures. Meanwhile, it is also confirmed that MWNTs can effectively improve the conductivity of the polymer matrix, resulting in the improvement of the electromagnetic interference shielding performance.[12–14]

Although many reports are available on the mechanical properties of the CNTs reinforced composites, there are very few reports on improving the electrical and thermal properties of these composites. The synthesis methods of CNT-reinforced composites primarily include ball milling, precipitation, sol-gel, in-situ methods, etc. Uniform dispersion of CNTs is achieved to a certain extent following these methods. However, in some cases, no improvement is seen in composites' properties. Momohjimoh et al. prepared 2 wt.% CNT-reinforced alumina (CNT/Al_2O_3) composites by the ultrasonic ball milling method. An increase in the conductivity from 10^{-13} S/cm (pure Al_2O_3) to 1.01 S/cm was observed. Liu et al. prepared the CNT/Al_2O_3 composites following the 3D extrusion printing technique. The material exhibited a conductivity of 10^{-1} S/m.[15,16] However, Lanfant et al. reported a significant decrease in the resistivity of the CNT-reinforced ceramic matrix composites. Zhan et al. adopted the method of spark plasma sintering to prepare single-walled CNT/Al_2O_3 composites and found that addition of CNTs results in the lowering of the thermal conductivity of the Al_2O_3 matrix.[17,18] It has been reported that the improvement in the composites' performance primarily depends on three aspects: (a) agglomeration and re-agglomeration, (b) structural integrity of the CNTs in the matrix, (c) interface bonding between CNTs and the matrix.[19–23]

To address these issues, spherical multi-wall carbon nanotube-reinforced alumina matrix (MWNT/Al_2O_3) composite powders were prepared by the sol-spray method. Further, the powders were sintered by a vacuum hot pressing (HP). Finally, the performance and microstructures of the composite materials are analyzed and discussed.

Experimental

Spherical MWNT/Al_2O_3 materials were prepared following the procedure as given in the schematic (Fig. 1). A certain amount of Al (NO_3)•$9H_2O$ was dissolved in deionized water, and MWNTs with a mass fraction of x (x = 0.0, 0.1, 0.5, 1.0, 2.0, and 4.0 wt.%) were added. This mixture was ultrasonicated for 30 mins. During magnetic stirring, ammonia water was slowly dripped to adjust the pH value of the solution (~ 7.0), which yielded a dilute colloidal precursor solution of water, aluminum hydroxide, and MWNTs. Adding ammonia water to the mixture of aluminum nitrate and MWNTs resulted in hydrated aluminum hydroxide colloids, which may be attached or coated on the MWNTs surfaces. The colloids with different viscosities could be obtained by adjusting the pH value of the solution. The precursor solution was then sprayed and pyrolyzed at 300°C to obtain the spherical composite powders (MWNTs coated with hydrated aluminum hydroxide). Then, the composite powder was thermally treated for 6 h under an argon atmosphere at 900°C. When crystalline water was removed from the hydrated aluminum hydroxide sample, the spherical MWNT/Al_2O_3 composite powders were obtained (Fig. 2c and d). Finally, the composite powder was sintered at 1500°C, 50 MPa for 1 h with HP. (HP HIGH-MULTI 500, Fuji Electric Industrial Co., Ltd.), and then cooled naturally.[24,25] The diameter and height of the final sample are about 10 mm and 2 mm after polishing, respectively.

The micromorphology and phases of the samples were analyzed by a JSM-7800F field emission scanning electron microscope (FESEM, JEOL, Japan) and an Ultima IV multi-function powder x-ray diffractometer (XRD, Rigaku Corporation, Japan). The Vickers hardness was measured using an FLC-50V Vickers hardness tester (FUTURE-TECH, Japan) with a 2 kg load (applied for 12 s), and

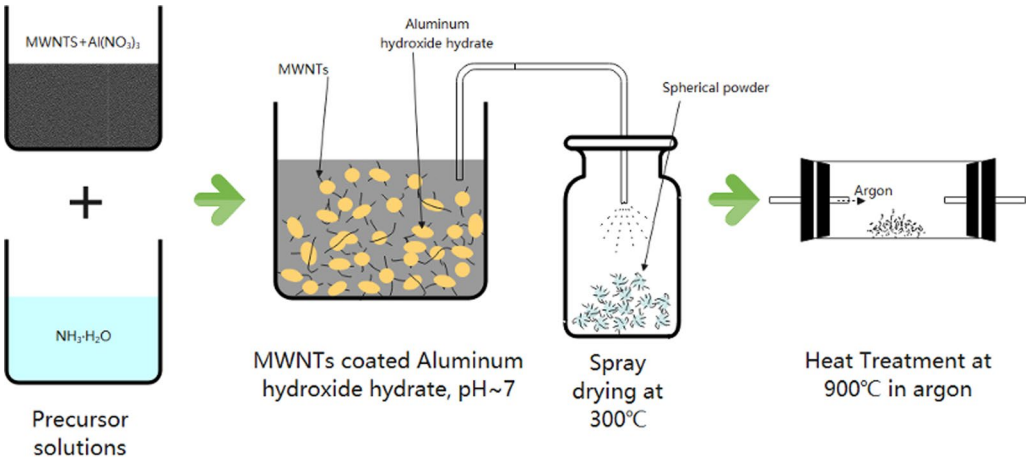

Fig. 1 Schematic of MWNT/Al_2O_3 spherical composite powder preparation.

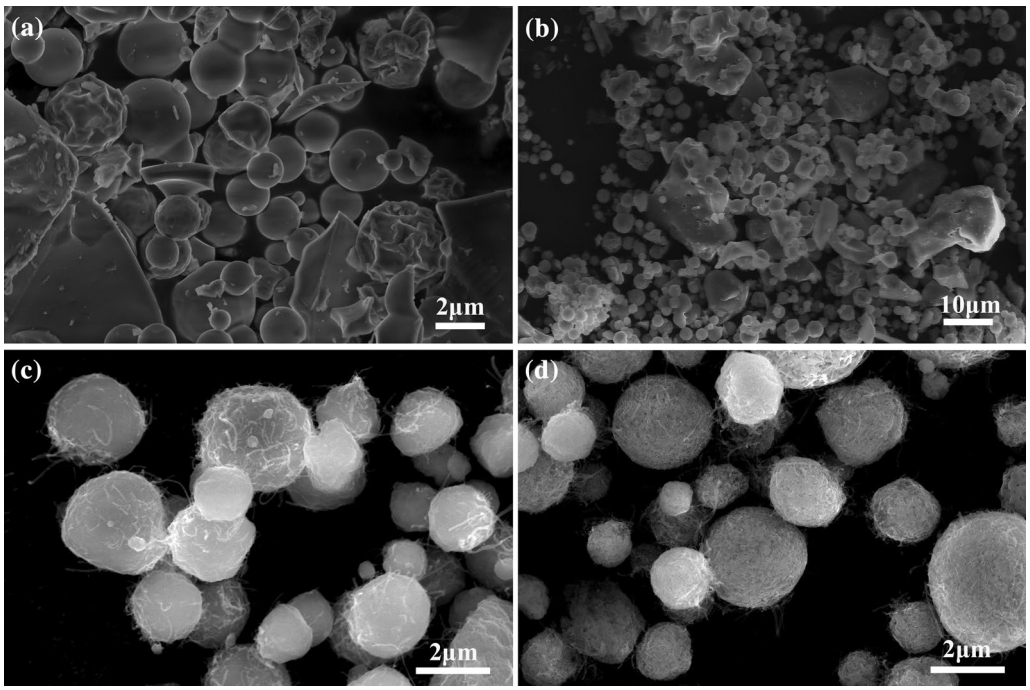

Fig. 2 SEM images recorded for the pure alumina and 1.0 wt.% MWNT/Al_2O_3 spherical composite powder; (a), (c) after spray drying at 300°C; (b), (d) after thermal treatment at 900°C in argon.

the average of 10 values was taken as the hardness (corresponding to each sample).[26] The fracture toughness of the nanocomposites was evaluated with the Antis equation.[27] The thermal diffusivity of the sample was measured by a laser thermal conductivity tester (Netzch LFA457, Germany) in the temperature range of 50-500°C. The conductivity of the composites was measured using an ST2253 digital four-probe tester, and the average value of 50 measurements under forward and reverse direct current (DC) is recorded.

Results and Discussion

Figure 2 displays the SEM images of the pure alumina and 1.0 wt.% MWNT/Al_2O_3 spherical composite powder prepared by the sol-spray technique. The spherical powders have a smooth surface without pores owing to their crystalline water (in Fig. 2a and c). However, the uneven surface of spherical composite powder contains numerous pores after thermal treatment at 900°C in the argon

atmosphere, which are caused by the loss of crystalline water from the colloid (Fig. 2b and d). Figure 3 shows the SEM images of the fracture surfaces of pure Al_2O_3 and 0.5 wt.% and 1.0 wt.% MWNT/Al_2O_3 composites. It can be seen that the 0.5 wt.% MWNTs are well distributed in the Al_2O_3 matrix with no obvious agglomeration, while a small amount of MWNTs agglomerated in 1.0 wt.% MWNT/Al_2O_3 composites. As shown in Fig. 3b and c, the MWNTs are primarily distributed along the grain boundaries, and some of the MWNTs pass through the Al_2O_3 grains, which can be analyzed base on the holes in the fracture surface (Fig. 3d). It is seen that the addition of MWNTs results in the refinement of the grain sizes of the composites because the network-shaped distribution of MWNTs inhibits grain growth in the composites. Statistical results show that the grain size of 0.5 wt.% MWNT/Al_2O_3 composites is approximately 1/3 of the sintered pure alumina sample.

The XRD patterns recorded for the MWNT/Al_2O_3 composites with different mass fractions are shown in Fig. 4. The main phase of the MWNT/Al_2O_3 composites is α-Al_2O_3. The results show that the (104) diffraction peaks of the composites are gradually shifted to higher angles with the content of MWNTs, which means that the lattice constant of this alumina matrix becomes smaller. This may be caused by the alumina grain refinement due to the addition of MWNTs. Figure 5 shows the Raman spectrum of the original MWNTs and 1.0 wt.% MWNT/Al_2O_3 composites. The G-band peak

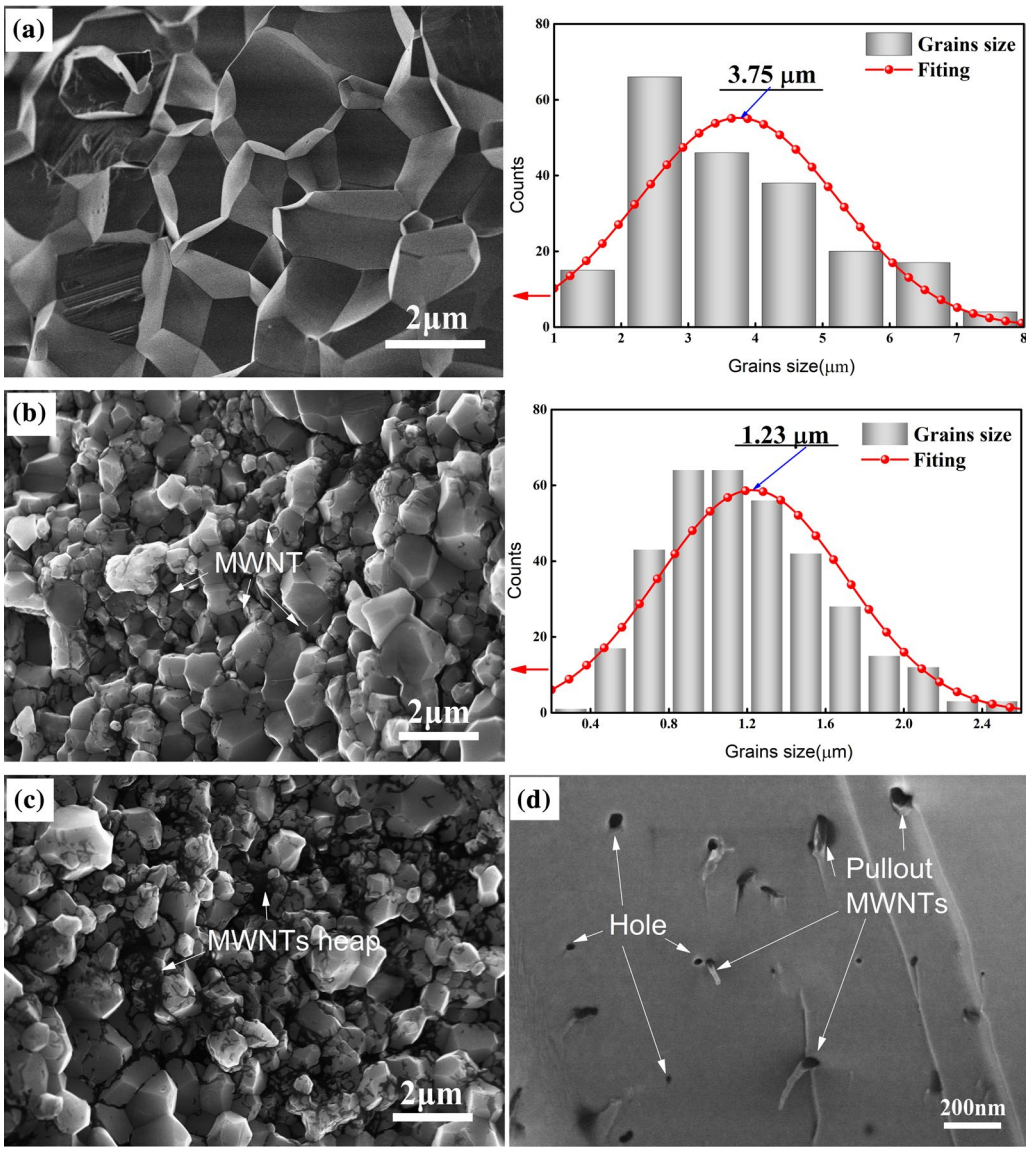

Fig. 3 SEM images of the fracture surfaces: (a) pure alumina; (b) and (d) 0.5 wt.% MWNT/Al_2O_3; (c) 1.0 wt.% MWNT/Al_2O_3.

indicates a highly ordered CNT sidewall, and D-band peak indicates disordered CNT sidewalls. Thus, the ratio of *D* and *G* band intensity (I_D/I_G) can reflect the graphitic feature of MWNTs. In this paper, the I_D/I_G ratio of the original MWNTs and 1.0 wt.% MWNT/Al_2O_3 composites are 0.68 and 0.81, respectively, which means that partial deterioration of the MWNTs sidewalls at high temperatures during the HP is not conducive to improving the composites' performance.

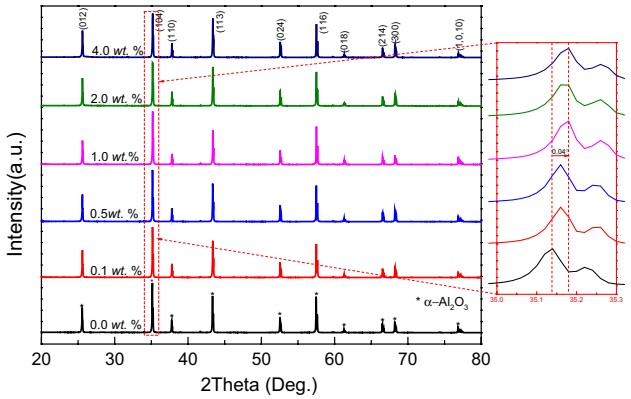

Fig. 4 XRD spectral profiles recorded for MWNT/Al_2O_3 composites with different mass fractions of MWNTs.

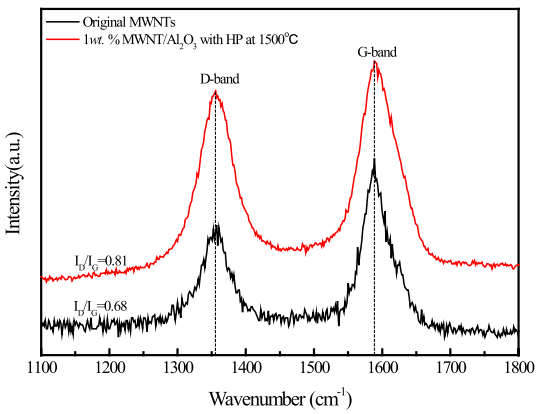

Fig. 5 Raman spectrum of original MWNTs and 1.0 wt.% MWNT/Al_2O_3 composites.

Table I shows the performance test results of the MWNT/Al_2O_3 composites. The relative density values of all samples are higher than 97.0%, which can be regarded as near full densification for a ceramic material. With the increase of MWNT-content, the relative density decreases. The maximum Vickers hardness and fracture toughness is achieved with 0.5 wt.% MWNTs, which are approximately 32.6% and 75.6% higher than those of pure Al_2O_3, respectively. This is because MWNTs refine the alumina matrix grains and are uniformly dispersed in the matrix without accumulation. However, with the increase of MWNT content, the Vickers hardness and fracture toughness of the composites gradually decrease. The fracture toughness of the composites is only 3.81 MPa•$m^{1/2}$ with 4.0 wt.% MWNTs. As the content of MWNTs increases, MWNTs are gradually accumulated at the grain boundaries of the matrix (in Fig. 3c), which deteriorates the properties of composites materials. The electrical conductivity results showed that the composites behaved as conductors when the MWNT content was higher than 0.5 wt.%. Moreover, the electrical conductivities of the composites are increased gradually with the MWNT content.

The electrical conductivity model of the composites is typically explained by the percolation theory, which shows that the conductivity largely depends on the mass fraction and length-width ratio of the conductive phase.[28,29] When the mass fraction of the conductive phase is low, the distance between the conductive phases is large, which reduces the contact between them and hinders the formation of the conductive path. In this case, the composites exhibit a low conductivity and act as an insulator. When the mass fraction of the conductive phases increases, the distance between the conductive phases decreases. There exists a critical concentration f_c. When the mass fraction of the conductive phases (f_{wt}) is greater than f_c, a conductive network across the insulating matrix is formed by the conductive particles. Under these conditions, the conductivity of the composites increases sharply. It is comparatively easy for the CNTs with a high length-to-diameter ratio to form conductive network paths in the matrix. This critical mass fraction of the conductive phases f_c is the critical percolation threshold. The

Table I Performance test results of MWNT/Al_2O_3 composites

Materials and HP parameters	Relative density (%)	Vickers hardness (HV)	Fracture toughness (MPa•$m^{1/2}$)	Electrical conductivity (S/cm)
0.0 wt.% MWNTs (1500°C, 50 MPa, 1 h)	100	1416.7	3.08	~10^{-13}
0.1 wt.% MWNTs (1500°C, 50 MPa, 1 h)	99.3	1493.7	3.62	–
0.5 wt.% MWNTs (1500°C, 50 MPa, 1 h)	98.4	1871.4	5.41	0.649
1.0 wt.% MWNTs (1500°C, 50 MPa, 1 h)	98.1	1703.6	5.27	0.838
2.0 wt.% MWNTs (1500°C, 50 MPa, 1 h)	98.0	1638.6	4.74	0.983
4.0 wt.% MWNTs (1500°C, 50 MPa, 1 h)	97.0	1233.2	3.81	1.144

conductivity of the composites increases exponentially, which can be expressed as follows:[30]

$$\sigma_m = \sigma_c \left(f_{\mathrm{wt}} - f_c\right)^t \left(f_{\mathrm{wt}} < f_c\right) \quad (1)$$

$$\sigma_m = \sigma_i \left(f_c - f_{\mathrm{wt}}\right)^{-s'} \left(f_{\mathrm{wt}} < f_c\right) \quad (2)$$

where σ_m is the DC conductivity of the composites, σ_c and σ_i are the DC conductivities of the conductor and insulator, respectively, f_{wt} and f_c are the mass fraction and percolation threshold of MWNTs, respectively, and t and s' are the conductivity indices.

Figure 6 shows the fitted results of the conductivity data given in Table I. The data were fit using Eqs. 1, 2, and the nonlinear least square method. The percolation threshold of the prepared composites can be expressed as $f_c \approx 0.37 \pm 0.07$ wt.%. The percolation threshold indicates the critical value corresponding to which the composites transits from an insulator to a conductor. The fitted percolation threshold f_c varies with the synthesis method. However, the fitted percolation threshold can accurately predict the dispersion of the conductive reinforcement phases in the matrix. Specifically, a smaller f_c corresponds to a more uniform dispersion of the reinforcement phase. In the present study, the fitted percolation threshold of MWNT/Al_2O_3 composites prepared by the sol–spray method is given by $f_c = 0.37 \pm 0.07$ wt.%. This indicates that the MWNTs are finely dispersed in the Al_2O_3 matrix.

Figure 7 shows the relationship between the thermal diffusivity and the content of MWNTs in the composites. With an increase in the MWNTs content, at first, the thermal diffusivity of the composites increases and then decreases under conditions of varying temperatures. The optimum value is achieved when the mass fraction is 0.5 wt.%. The thermal conduction mechanism of the composites materials primarily depends on electron motion and phonon vibration. In addition, the photons participate at high temperatures. For pure Al_2O_3-based ceramics, the primary thermal conduction mechanism is phonon vibration. With the addition of MWNTs, a hybrid mode of thermal conduction is observed in the composites (see Fig. 3b), which includes phonon vibration and electron motion.[31,32] From Fig. 5, it can be seen that when the MWNT content (0.1 wt.%) is less than f_c, the thermal diffusivity of the composites (with phonon vibration as the primary thermal conduction mechanism) changes slightly; when the content of MWNTs is higher than f_c, many effective conductive networks are formed in the composite material, so the thermal diffusivity is composed of phonon vibration and electron motion. When the content of MWNTs is 0.5 wt.%, the maximum thermal diffusivity of composites is obtained under conditions of varying temperatures. When the content of MWNTs is higher than 0.5 wt.%, the thermal diffusivity of the composites shows a downward trend. This is because when the content of MWNTs is 0.5 wt.%, the MWNTs in the composite material are uniformly distributed without accumulation. When the content of MWNTs gradually increases, the accumulation of MWNTs in the matrix (see Fig. 3c) causes the relative density of the composite material to decrease, and pores appear, which affects the phonon thermal conductivity of the matrix.

Table II shows the thermal diffusivities of the pure alumina and 0.5 wt.% MWNT/Al_2O_3 composites under conditions of varying temperatures. An average increase of 26.2%

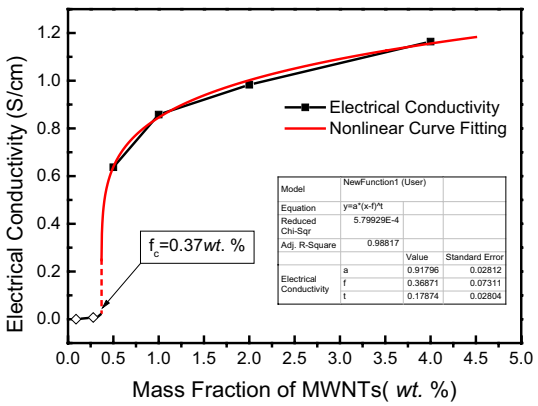

Fig. 6 Fitted curve of the electrical conductivity with the data in Table I.

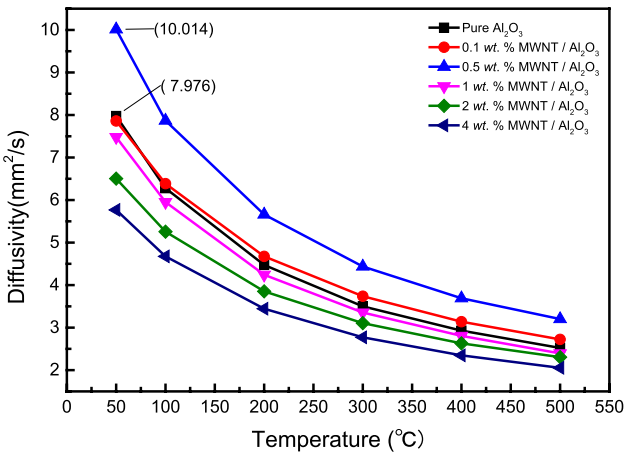

Fig. 7 Relationships of the thermal diffusivity and MWNT content at different test temperatures.

Table II Thermal diffusivity of the 0.5 wt.% MWNT/Al_2O_3 composites and pure Al_2O_3 at different test temperatures

Test temperature (°C)	Thermal diffusivity of pure Al_2O_3 (mm^2/s)	Thermal diffusivity of 0.5 wt.% MWNT/Al_2O_3 (mm^2/s)	Increase of thermal diffusivity (%)
50	7.976	10.014	25.6
100	6.278	7.868	25.3
200	4.473	5.660	26.5
300	3.500	4.437	26.8
400	2.929	3.690	26.0
500	2.522	3.201	26.9
Average value			~26.2

is seen in the case of the 0.5 wt.% MWNT/Al_2O_3 composites (compared to the value recorded for the pure alumina matrix), which can be attributed to the excellent thermal diffusivity of the MWNTs.

Conclusion

Spherical MWNT/Al_2O_3 composite powders were prepared following the sol-spray method. The MWNTs were well dispersed in the matrix and this method is also time for mass production. Optimum properties were obtained when 0.5 wt.% of MWNTs were added. Specifically, the relative density was as high as 98.7%, the Vickers hardness and fracture toughness increased by 32.1% and 75.6%, respectively, the average increase in thermal diffusivity was 26.2% (compared to values recorded for the pure Al_2O_3 matrix). The percolation threshold of the composites was fitted as $f_c \approx 0.37 \pm 0.07$ wt.%. This also indicated that the MWNTs in the composites prepared following the sol-spray method were uniformly dispersed. This study focused on the physical properties and the electrical and thermal conductivities of the MWNT/Al_2O_3 composites. As the surface wettability between the CNTs and Al_2O_3 is poor, research to improve the interfacial bonding can be conducted in the future. The interfacial bonding can be potentially improved by adding a transition layer like SiO_2 or ZrO etc.

Acknowledgments This work is supported by the Chinese National Science Foundation (Grant No. 52064032, 52174345), and the Yunnan Science and Technology Projects Grants (Grant No. 2019ZE001, 202002AB080001).

Conflict of interest On behalf of all authors, the corresponding author states that there are no conflicts of interest.

References

1. S. Iijima, *Nature* 354, 56 (1991).
2. C. Ke, C.C. Jia, and W.S. Li, *Appl. Phys. A* 110, 269 (2013).
3. K.F. Chan, M. Zaid, M.S. Mamat, S. Liza, and Y. Yaakob, *Curr. Comput.-Aided Drug Des.* 11, 457 (2021).
4. S.S. Park, M.S. Moorthy, and C.S. Ha, *Korean J. Chem. Eng.* 31, 1707 (2014).
5. R.U. Hassan, F. Shahzad, N. Abbas, and S. Hussain, *J. Mater. Sci-Mater El.* 30, 6304 (2019).
6. J.R. Martinelli, and F.F. Sene, *Ceram. Int.* 26, 325 (2000).
7. H.J. Kim, J.H. Kim, K.W. Jun, J.H. Kim, W.C. Seung, O.H. Kwon, J.Y. Park, S.W. Kim, and I.K. Oh, *Adv. Energy Mater.* 6, 8 (2016).
8. C. Li, T. Liang, W. Lu, C. Tang, X. Hu, M. Cao, and L. Ji, *Compos. Sci. Technol.* 64, 2089 (2004).
9. T.-H. Lee, S.-H. Cho, T.-G. Lee, H.T. Kim, I.-K. You, and S. Nahm, *J. Am. Ceram. Soc.* 101, 7 (2018).
10. D.L. Chung, *Carbon* 39, 279 (2001).
11. M.A. Singh, D.K. Sarma, O. Hanzel, J Sedlá?Ek, and ?ajgalík, *J. Eur. Ceram. Soc.* 37, 3107 (2017). https://doi.org/10.1016/j.jeurceramsoc.2017.03.058.
12. C.H. Kuo, and H.M. Huang, *J. Therm. Anal. Calorim.* 103, 533 (2011).
13. B. Lanfant, Y. Leconte, N. Debski, G. Bonnefont, and F. Bernard, *Ceram. Int.* 45, 2566 (2019).
14. A.B. Kaiser, and G.S. Düsberg Roth, *Phys. Rev. B* 57, 1418 (1998).
15. I. Momohjimoh, N. Saheb, M.A. Hussein, T. Laoui, and N. Al-Aqeeli, *Ceram. Int.* 46, 16008 (2020).
16. B. Lanfant, Y. Leconte, N. Debski, M. Pinault, M. Mayne, N. Herlin, G. Bonnefont, V. Garnier, Y. Jorand, and G. Fantozzi, *TechConnect World, Washington* (2014). https://www.hal.univ-lille.fr/LFP-CEA/hal-01095227
17. C. Liu, and J. Ding, *Procedia Manuf.* 48, 763 (2020).
18. G.D. Zhan, and A.K. Mukherjee, *Int. J. Appl. Ceram. Tec.* 1, 161 (2010).
19. N. Saheb, and U. Hayat, *Ceram. Int.* 43, 5715 (2017).
20. K. Lee, B.M. Chan, S.B. Park, and S.H. Hong, *J. Am. Ceram. Soc.* 94, 3774 (2011).
21. L. Kumari, T. Zhang, G.H. Du, W.Z. Li, Q.W. Wang, A. Datye, and K.H. Wu, *Ceram. Int.* 35, 1775 (2009).
22. M. Estili, and Y. Sakka, *Sci. Technol. Adv. Mat.* 15, 064902 (2014).
23. S.C. Zhang, W.G. Fahrenholtz, G.E. Hilmas, and E.J. Yadlowsky, *J. Eur. Ceram. Soc.* 30, 1373 (2010).
24. S.M. Barinov, L.V. Fateeva, S.V. Yurashev, B. Ballóková, and E. Rudnayová, *Powder Metall. Prog.* 2, 4 (2002).
25. J. Lin, G. Fan, Z. Li, X. Kai, Z. Di, Z. Chen, S. Humphries, G. Heness, and W.Y. Yeung, *Carbon* 49, 1965 (2011).
26. Viana, Bruno, Zych, Eugeniusz, Gao, Yun, Chen, Wei, Peng, and Mingying, A Special Issue on Functional Nanomaterials and Applications (2017). https://doi.org/10.1166/jnan.2014.1214.
27. X. Wang, and A. Atkinson, *J. Eur. Ceram. Soc.* 35, 3713 (2015).

28. P.M. Groffman, J.S. Baron, T. Blett, A.J. Gold, I. Goodman, L.H. Gunderson, B.M. Levinson, M.A. Palmer, H.W. Paerl, and G.D. Peterson, Ecological Thresholds (2006). https://www.xueshu.baidu.com/usercenter/paper/show?paperid=d04d52516983035f936db3a00480fe04&site=xueshu_se.
29. M. Sahimi, Percolation Processes (American Cancer Society, 2003). https://doi.org/10.1002/3527600434.eap581.
30. D.J. Bergman, *Phys. Rev. Lett.* 44, 1285 (1980).
31. N. Cewen, *Prog. Mater. Sci.* 37, 1 (1993).
32. Y. Ben-Menahem, and M. Hemmo, *Probability in Physics* (Berlin Heidelberg: Springer, 2012).

Authors and Affiliations

Songlin Tan[1] · Rui Bao[1] · Yongqi Zhuang[1] · Jianhong Yi[1]

✉ Songlin Tan
20060051@kust.edu.cn

[1] Faculty of Materials Science and Engineering, Kunming University of Science and Technology, Kunming 650093, China